

Article

Analysis of a Modified Y-Branch CWDM Demultiplexer Based on Photonic Crystal Structure

Oualida El Mansouri¹ , Amel Labbani¹ 

¹Laboratory of Hyperfrequency and Semiconductors, Department of Electronics, Faculty of Technology Sciences, University of Mentouri Brothers Constantine 1, Constantine, Algeria. elmansouri.oualida@umc.edu.dz and labbani.amel@umc.edu.dz.

Abstract—This paper attempts to investigate the design of a modified Y-shaped demultiplexer based on photonic crystal. The designed structure is used to select four telecommunication wavelengths. In our design, four resonant cavities (RC) are utilized. A square lattice of silicon (Si) rods immersed in air matrix is used as a fundamental structure. Thus, our study is to investigate the effect of various design parameters on the output frequency. To simulate the performance of the proposed device, the Finite Difference Time Domain (FDTD) approach is used. The obtained results show that the average power transmission, quality factor, channel spacing, crosstalk, and full width at half maximum, are 99.925 %, 4638.785, 19.6 nm, from -40,119 to -24,316 dB, and 0.325 nm, respectively. Additionally, the proposed demultiplexer is very compact with a total footprint of 269 μm^2 , which is very suitable to be utilized in compact photonic integrated circuits (PIC).

Index Terms—Crosstalk, Demultiplexing, Photonic crystals, Telecommunication system.

I. INTRODUCTION

The rise of high-speed internet and the increasing demand for connectivity have led to the development of advanced technologies, such as Fiber-to-the-Home (FTTH), which provide high-speed communication services directly to households. In these modern networks, Coarse Wavelength Division Multiplexing (CWDM) demultiplexers play a crucial role in optimizing the utilization of optical infrastructure [1]-[3].

In telecommunication networks, optical filters and demultiplexers play pivotal roles, particularly in Wavelength Division Multiplexing (WDM) and Coarse Wavelength Division Multiplexing (CWDM) systems. Optical filters are essential components tasked with selecting specific wavelengths from a multitude of frequencies without interfering with other channels transmitted through the fiber.

Meanwhile, optical demultiplexers are specialized devices engineered to separate a composite optical signal into its individual components, often based on their respective wavelengths, utilizing a combination of multiple filters. By extracting each channel separately, demultiplexers facilitate

precise signal processing and analysis, thereby contributing to the maintenance of optimal network performance [4],[5].

CWDM optical demultiplexers are of great importance in modern communication networks due to their numerous advantages. They enable the efficient use of optical bandwidth by multiplexing and demultiplexing multiple channels at different wavelengths on a single optical fiber. The significance of CWDM demultiplexers lies in their ability to increase network capacity while minimizing investment costs. With well-established international standards, such as ITU-T G.694.2, CWDM demultiplexers ensure seamless interoperability between different equipment and manufacturers, which facilitate their widespread deployment. The wavelength ranges used in CWDM demultiplexers (1271-1611 nm), typically spaced 20 nm apart, allow for effective bandwidth allocation and the harmonious coexistence of multiple channels on a single optical fiber [6],[7]. Moreover, CWDM demultiplexers based on photonic crystals offer significant advantages over conventional demultiplexers. These innovative devices are to exploit the unique optical properties of photonic crystals to efficiently separate signals at different wavelengths on a single optical fiber [8].

One of the main advantages of photonic crystal-based CWDM demultiplexers is their superior spectral selectivity and channel separation precision. Unlike conventional demultiplexers, which can suffer from interference and crosstalk issues between channels, photonic crystal-based demultiplexers ensure reliable and undisturbed transmission of signals at different wavelengths [9].

Another key advantage is the compactness of these demultiplexers. The advanced design of photonic crystals and their ability to be miniaturized enable their integration into small-sized devices. This facilitates their seamless integration into existing communication systems without requiring major infrastructure modifications, making them particularly valuable in space-constrained environments [10], [11].

Furthermore, photonic crystal-based CWDM demultiplexers exhibit lower insertion losses compared to conventional demultiplexers. This low insertion loss enhances energy efficiency and enables data transmission over longer distances with high signal quality.

Lastly, their superior thermal stability is a crucial advantage. Photonic crystal-based CWDM demultiplexers maintain their performance even in the presence of temperature variations, ensuring consistent and reliable data transmission under changing conditions [12].

Knowing the importance and advantages of demultiplexer, in this study we propose a demultiplexer that can operate within the telecommunications CWDM C-band (1470-1610 nm), and even in the S-band (1460-1530 nm), which lies on the shorter wavelength side of the C-band with an average spacing of 18 nm, as demonstrated by the fundamental structure of the filter. Our study presents a new

structure of a four-wavelength CWDM demultiplexer, consisting of four resonant cavities. The positive simulation result's, such as the quality factor and transmission efficiency, highlight the various advantages obtained from this approach.

II. BASIC PHOTONIC CRYSTAL DESIGN

The primary proposed structure consists of a square lattice of silicon (Si) rods with refractive index $n_r=3.43$ in an air background ($n_s=1$). The number of circular rods in x and z directions is 31 and 43, respectively. The radius of the Si rods is set to be $0.21a$, where a is the lattice constant of the structure. We calculated the photonic band gap (PBG) using the PWE approach [13]-[15], the dispersion diagram is shown in Fig. 1. This figure illustrates that the proposed device has two PBGs operating in transverse electric (TE) mode, while, there is no PBG in the TM mode. The first PBG is observed from 0.28583 (a/λ) to 0.42047 (a/λ), where λ is the vacuum wavelength. The obtained PBG is large enough to cover the necessary frequencies for optical communication applications and has a suitable wavelength range for our objectives.

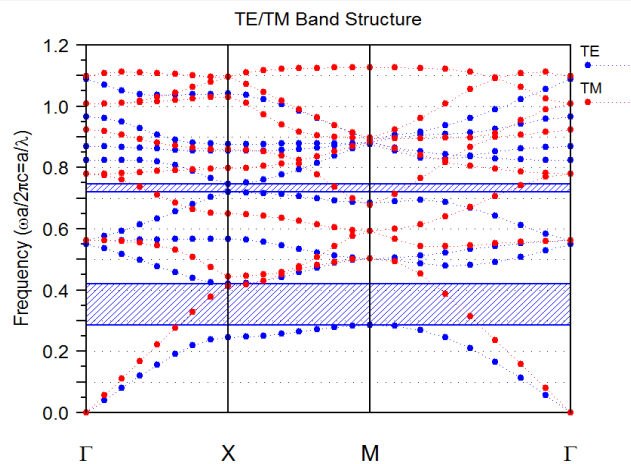


Fig. 1. Band diagram of Si rods arranged in air background for TE polarization.

III. SIMULATION AND ANALYSIS

A. Filter design

To design our filter, we create two linear waveguides by removing a series of dielectric rods in the x direction. They are connected to each other via a resonant cavity. The input waveguide is formed by omitting 8 dielectric rods in the ΓX direction, while the output one is obtained by removing 7 particles in the same direction. The RC is created by removing five dielectric rods. As shown in Fig. 2, the radius of the defect rods located at the top and the bottom of the cavity are set to be $0.31a$. They are denoted as r_c . While the two coupling rods which are positioned horizontally at the edge of the cavity, are highlighted by r_{cp} . The RI of the matrix, defect and coupling rods are labeled as, n_r , n_c , n_{cp} respectively. Modifying the optical parameters of photonic crystal structures generally results in changes to their optical properties. Our objective in this section is to investigate the effect of n_c , r_c and r_{cp} on the resonant mode of the RC.

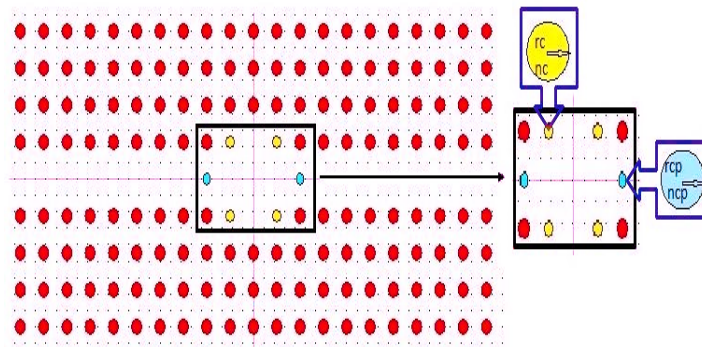


Fig. 2. Schematic diagram of the proposed filter.

One of the most important characteristics of the filter is its tunability. So, in this section, we investigate how a specific structural parameter, rc impacts the filtering feature of the structure. By varying the values of rc , we can achieve different resonant wavelengths. Fig. 3, illustrates that for $rc = 0.167 a$, $0.171 a$, $0.173 a$, $0.175 a$, $0.177 a$, $0.178 a$, and $0.182 a$, the output spectra of the suggested filter can isolate distinct resonant wavelengths $1.4739 \mu\text{m}$, $1.4810 \mu\text{m}$, $1.4841 \mu\text{m}$, $1.4861 \mu\text{m}$, $1.4887 \mu\text{m}$, $1.4902 \mu\text{m}$ and $1.4983 \mu\text{m}$, respectively. We noticed that the highest Q factor of 3715.25 is achieved when $rc=0.175 a$. In addition, an average transmission efficiency of 98.28 is attained. We studied another parameter that affects the output transmission spectrum of the filter. This parameter is the coupling rods rcp . We investigate the change of rcp from $0.156 a$ to $0.289a$. The calculated Q factor for this case is 4978.7. According to Fig. 4, it has been observed that an increase in rcp moves the output signal to lower frequency. Similarly, the refractive index variation of the defect rods from 3.4 to 3.48 is also analyzed. It can be seen from Fig. 5 that the displacement of the resonant mode is strongly affected by the change of the RI of the coupling rods. The variation of the refractive index of rc can be obtained by employing electro-optic or thermo-optic material. This result indicates that the structure can be adjusted to achieve the appropriate frequency of the filter.

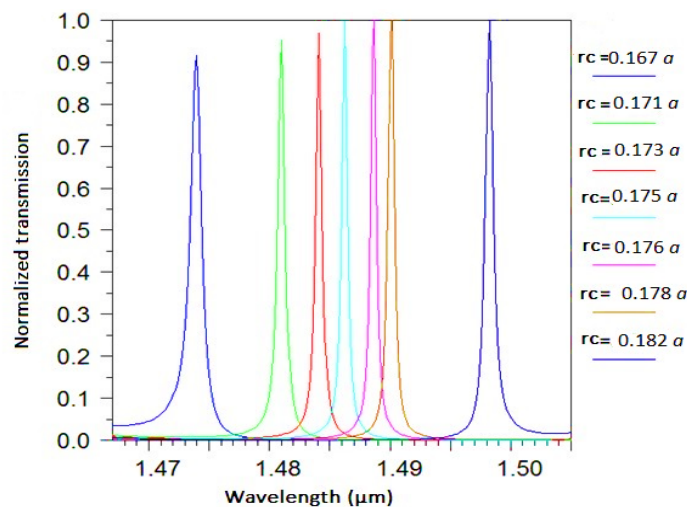


Fig. 3. Normalized transmission spectra of the proposed filter for different values of defect rods rc .

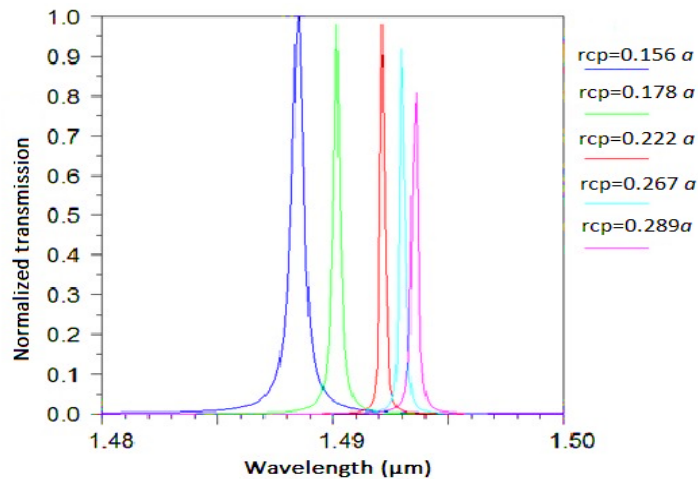


Fig. 4. Normalized transmission spectra of the proposed filter for different values of coupling rods r_{cp} .

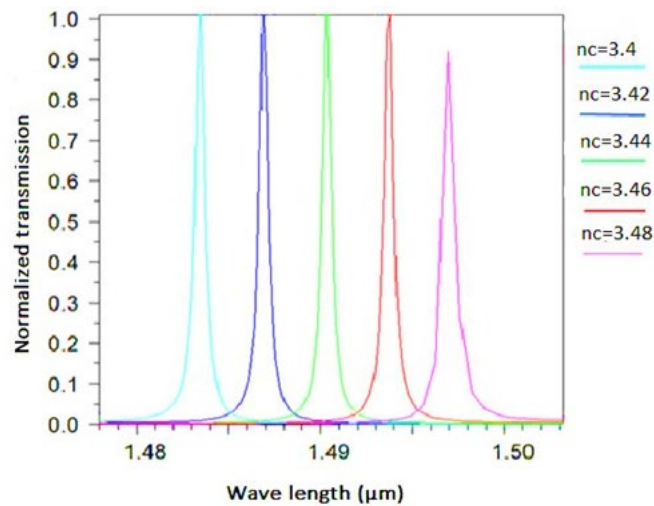


Fig.5. Normalized transmission spectra of the proposed filter for different values RI n_c .

B. Modified Y-branch demultiplexer design

The proposed demultiplexer consists of four parallel waveguides arranged in a modified Y-shaped 1x4 as shown in Fig. 6. When the electromagnetic wave is injected at the input waveguide, it is guided along the linear defect. At resonant wavelength, the propagating electromagnetic wave couples to the resonant modes of the cavities. Therefore, all the energy is extracted and detected through the output ports. To study the transmission properties of the proposed design, we used the FDTD method., The numerical simulation results show that the modified Y-shaped can separate four wavelengths in the telecommunications domain within the CWDM C-band (1470-1610 nm), and even in the S-band (1460-1530 nm), which lies on the shorter wavelength side of the C-band with an average spacing of 19.6 nm.

The normalized transmission (efficiency), wavelength spacing λ , and quality factor "Q" are the most important characteristics of the demultiplexer.

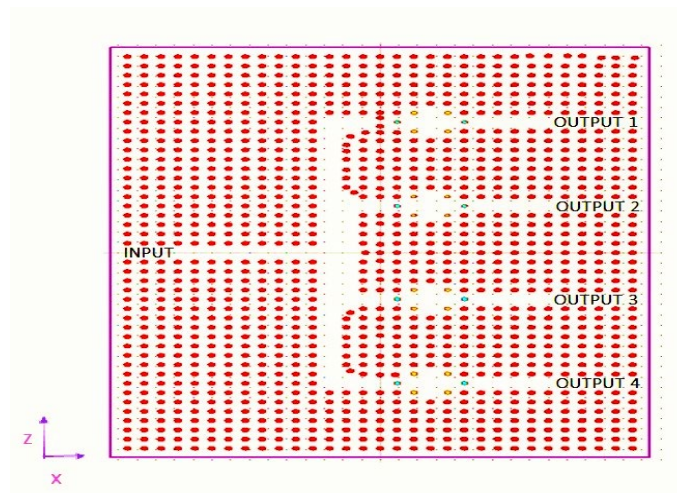


Fig.6. Schematic structure of the proposed demultiplexer.

The study of our demultiplexer begin by varying the radius r_c . Fig. 7 shows that for $r_c=0.188 a$, $r_c=0.177 a$, $r_c=0.173 a$ and $r_c=0.144 a$, the demultiplexer enables the selection of wavelengths $\lambda_1=1454.1$ nm, $\lambda_2=1474.1$ nm, $\lambda_3=1492.3$ nm, and $\lambda_4=1508.8$ nm respectively. To calculate the transmission spectrum and measure the transmitted power of the suggested design, four monitors were placed at the output ports 1, 2, 3, and 4.

A Gaussian-modulated pulse is launched at the input waveguide at wavelength 1550nm. The input light flow of the pulse travels through each cavity in which interact and get detected with the monitor placed at the output waveguide. The calculations were performed using the Fullwave module of the RSoft CAD software. As results we obtained an average values of quality factor, wavelength spacing, transmission efficiency and passband as 3176.87, 18.6 nm, 99.625, 0.6475nm respectively .

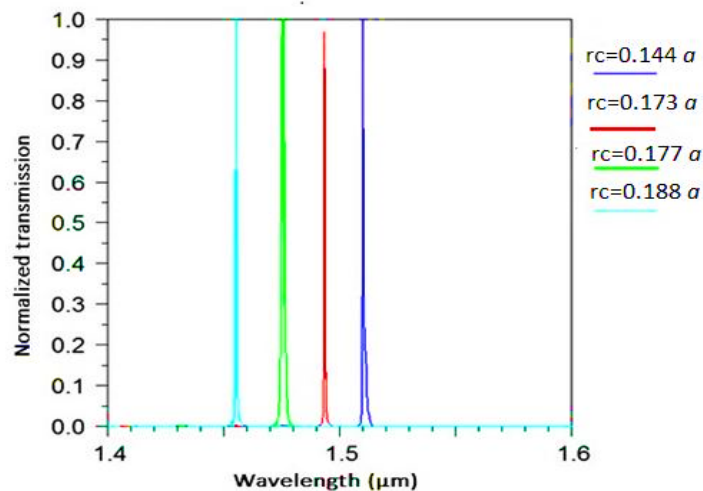


Fig. 7. Normalized transmission spectra of the proposed demultiplexer for different values of r_c .

Fig. 8 (a), Fig. 8 (b), Fig. 8 (c) and Fig. 8 (d) clearly show the distribution of the electric field in the suggested structure for the four wavelengths. This device enables the demultiplexing of the detected wavelengths, and their selection is clearly observed.

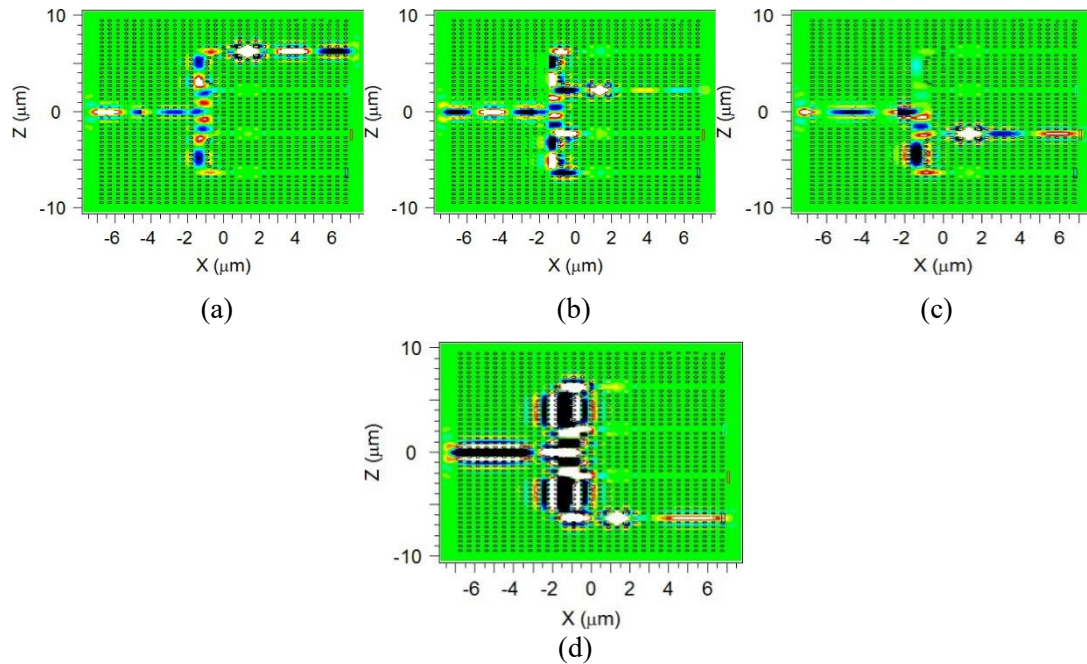


Fig.8. The distribution of the electric field in the proposed demultiplexer.
 (a) $\lambda_1=1454.1$ nm (b) $\lambda_2=1474.1$ nm (c) $\lambda_3=1492.3$ nm (d) $\lambda_4=1508.8$ nm.

By choosing different values for r_{cp} we can obtain different resonant wavelengths. As shown in Fig. 9, our proposed demultiplexer is simulated with different r_{cp} equal to $215a$, $217a$, $204a$, and $202a$, that can select wavelengths 1456 nm, 1494.8 nm, 1474.1 nm and 1510.2 nm, respectively. The obtained average values of quality factor, wavelength spacing, transmission efficiency and passband are respectively 4179.1, 17.86 nm, 97.95% and 0.425 nm.

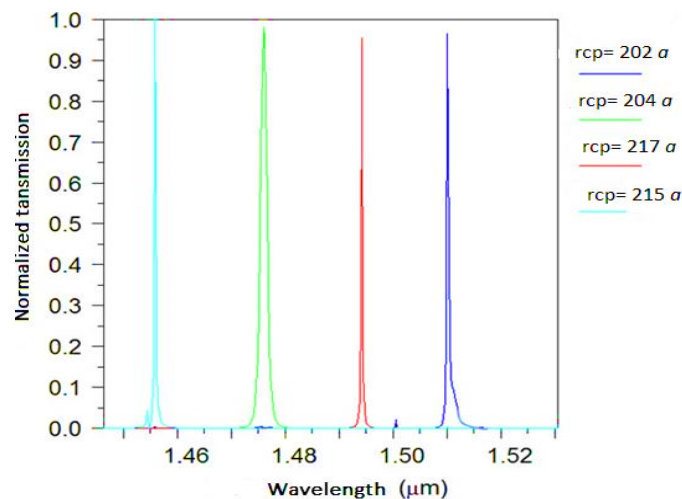


Fig.9. Normalized transmission spectra of the demultiplexer with different variation of r_{cp} .

In a similar manner as before, we studied another case for our periodic material-based demultiplexer. The frequency selection was achieved by varying the refractive index of the internal resonator particles. For indices $n_c=3.4$, $n_c=3.41$, $n_c=3.44$, and $n_c=3.45$, the suggested structure allows for the demultiplexing of four wavelengths: $\lambda_4=1493.6$ nm, $\lambda_2=1489.0$ nm, $\lambda_3=1491.8$ nm, and $\lambda_1=1487.1$ nm. They are

represented in Fig. 10. Average values of quality factor, wavelength spacing, transmission efficiency and passband are respectively 4638.7875, 19.66 nm, 99.925% and 0.325 nm.

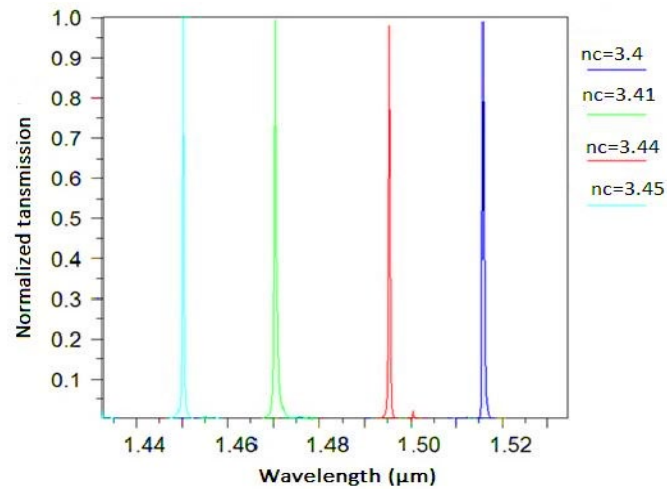


Fig. 10. Normalized transmission spectra of the demultiplexer for various refractive index n_c .

After performing various parameter variations of the demultiplexer, we observed that the variation of the refractive index n_c yields better results.

Crosstalk is a crucial aspect to consider when designing a demultiplexer. It is quantified using the crosstalk calculation formula [16]:

$$X(dB) = 10 \log \frac{(1 - A)}{(1 - A_i)} \quad (1)$$

In this equation, A represents the maximum transmission value of the resonant cavity for a specific channel at its resonant frequency, while A_i denotes the transmission value of the adjacent channels at the same resonant frequency. As the crosstalk decreases, the demultiplexer's resolution improves.

Fig. 11 illustrates the cross-talk rate in the 4-channel demultiplexer. The cross-talk rate of the channels is obtained, respectively, compared to each other, as shown in Table I. The highest inter-channel cross-talk is related to channels 1 and 3, and the lowest inter-channel cross-talk is related to channels 4 and 1.

TABLE I. CROSS-TALK RATES BETWEEN DIFFERENT CHANNELS IN THE 4-CHANNEL DEMULTIPLEXER

Channels Crosstalk (dB)	Ch 1	Ch 2	Ch 3	Ch 4
Ch 1	---	-27.593	-24.316	-29.366
Ch 2	-30.021	---	-29.29	-25.201
Ch 3	-37.775	-31.247	---	-30.864
Ch 4	-40.119	-29.569	-30.76	---

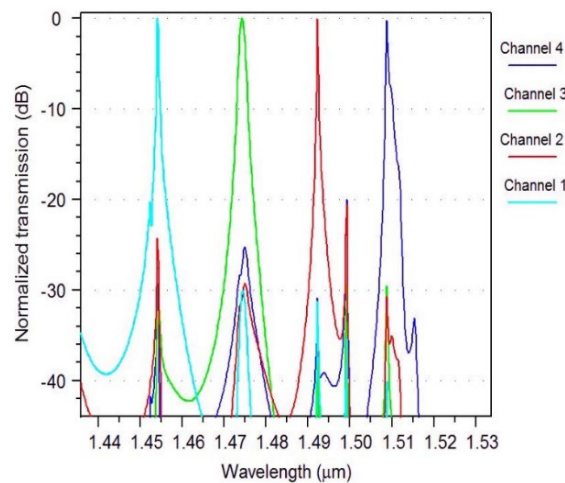


Fig. 11. Cross-talk diagram in the 4-channel demultiplexer.

The proposed structure exhibits a significant distinction by achieving an acceptable crosstalk level ranging from -40.119 dB to -24.316 dB between the outputs.

Table II represents a comparison between our results and some published articles. The efficiency, quality factor, and average spacing between the wavelengths of the proposed demultiplexer are very satisfactory.

Table II. Parameter comparison of some published paper

Reference	Channel number	Wavelength Used(nm)	Crosstalk (dB)	Efficiency (%)	Spacing (nm)	Q
[6] 2016	4	1510-1570	-10.135 to -26.072	80	20	225
[18] 2017	8	1542–1555	-18	99	1.75	4860
[7] 2018	8	1521.1- 1523.2	-3.4 to -26.9	98	1	1823
[19] 2022	8	1420–1460	-19.7 to-0.8	92	5.6	256
This Work	4	1450,5- 1510,4	-40,119 to -24,316	99.925	19.6	4638.78

IV. CONCLUSION

In this paper, we investigate a four –channel demultiplexer based on a modified Y-branch photonic crystal structure designed for CWDM (Coarse Wavelength Division Multiplexing) systems in both the C and S bands.

The suggested design enables the separation of four telecommunication wavelengths by adjusting different parameters of the resonant cavity. To separate the desired wavelengths, optical filters based on a resonant cavity are used. The optical filter designed has indeed a very favorable transfer coefficient and quality factor, with an average quality factor of 4638.785 and a transmission efficiency of 99.925%.

The proposed demultiplexer exhibits low crosstalk and a compact size of about $269 \mu\text{m}^2$, which makes it well-suited for photonic integrated circuits and future optical networks.

REFERENCES

- [1] A. Rostami, H. Alipour Banaei, F. Nazari, A. Bahrami, "An ultra compact photonic crystal wavelength division demultiplexer using resonance cavities in a modified Y-branch structure," *Optik*, vol 122, Issue 16, pp1481-1485, 2011.
- [2] R. K. Sinha, Swati Rawal, "Modeling and design of 2D photonic crystal based Y type dual band wavelength demultiplexer," *Optical and Quantum Electronics*, vol 40, pp 603–613, 2008.
- [3] Fiberdyne Labs. <http://www.fiberdyne.com/products/pdf/cwdmintr.PDF>. Cited 11 Sept 2007.
- [4] I. Moumeni and A. Labbani, "Very High Efficient of 1×2 , 1×4 and 1×8 Y Beam Splitters Based on Photonic Crystal Ring Slot Cavity," *Optical and Quantum Electronics*, vol. 53, no. 2, pp 1–15, 2021.
- [5] Rashki, Z., Seyyed Mahdavi Chabok, S. J., "Novel design of optical channel drop filters based on two-dimensional photonic crystal ring resonators," *Optics Communications*, vol 395, pp 231–235, 2017.
- [6] K. Venkatachalam, S. Robinson, S. Uma Maheswari, "Two Dimensional Photonic Crystal based Four Channel Demultiplexer for ITU.T.G 694.2," *International Journal of Photonics and Optical Technology*, vol 2, pp 37-41, 2016.
- [7] K. Venkatachalam, S. K Dhamodharan and S.Robinson, "Investigation of 2D-PC Ring Resonator-Based Demultiplexer for ITU-T G.694.1 WDM Systems," *Journal of Optical Communications*, May 2018.
- [8] Youssef Ben-Ali and al, "Two-Channel Demultiplexer Based on 1D Photonic Star Waveguides Using Defect Resonators Modes," *Progress In Electromagnetics Research B*, vol. 93, pp 131–149, 2021.
- [9] Bernier. D, X. Le Roux, A. Lupu, D. Marris-Morini, L. Vivien, and E. Cassan, "Compact low crosstalk CWDM demultiplexer using photonic crystal superprism," *Optics Express*, vol. 42, pp 17260– 17214, 2008.
- [10] Gholamali Delphi et al, "Design of low cross-talk and high-quality-factor 2-channel and 4-channel optical demultiplexers based on photonic crystal nano-ring resonator," *Photonic Network Communications*, vol 38, pp 250–257, 2019.
- [11] Masoud Mohammadi, Mahmood Seifouri, "A new proposal for a high-performance 4-channel demultiplexer based on 2D photonic crystal using three cascaded ring resonators for applications in advanced optical systems," *Optical and Quantum Electronics*, vol 51, 350, 2019.
- [12] Saseendran, Swaran, Bhowmick, Kaustav; Sreenivasulu.T, "Design of photonic crystal based demultiplexer for CWDM technology," *IEEE International Conference on Advanced Networks and Telecommunications Systems (ANTS), 2017*.
- [13] Taflove, "The Finite- difference Time-domain Method", *Computational Electrodynamics*, Artech House, 1995.
- [14] Venkatachalam Rajarajan Balaji et al, "Optimization of DWDM Demultiplexer Using Regression Analysis," *Hindawi Publishing Corporation, Journal of Nanomaterials*, Special issue, 2016.
- [15] J. Clerk Maxwell, "A dynamical theory of the electromagnetic field," *Journal of Philosophical Transactions of the Royal Society of London*, vol. 155, no. 1865, pp 459–512, 2015.
- [16] Rajarajan B.V., Murugan M., Robinson S., Nakkeeran R., "Design and optimization of photonic crystal based eight-channel dense wavelength division multiplexing demultiplexer using conjugate radiant neural network," *Optical and Quantum Electronics*, vol 49 (198), pp 1–15, 2017.
- [17] Sanaa Ghezali et al, "Nine Channels Wavelength Division Demultiplexer Based upon Two Dimensional Photonic Crystal," *Progress In Electromagnetics Research M*, vol. 69, pp 107–114, 2018.
- [18] Talebzadeh.R, Soroosh.M, Kavian.Y.S, Mehdizadeh.F, "Eight-channel all-optical demultiplexer based on photonic crystal resonant cavities," *Optik*, vol 140, pp 331–337, 2017.
- [19] Venkatachalam.K, Sriram Kumar.D, Robinson.S, "Investigation on Ultra-Compact 2DPC Coarse Wavelength Division De-multiplexer," *Journal of Biopolymers and Theoretical Studies*, vol 2, pp 39-45, 2022.